Renormalized interactions with a realistic single particle basis

Angelo Signoracci[1], B. Alex Brown[1], and Morten Hjorth-Jensen[2]

[1]*Department of Physics and Astronomy and National Superconducting Cyclotron Laboratory, Michigan State University, East Lansing, Michigan 48824-1321, USA and*

[2]*Department of Physics and Center of Mathematics for Applications, University of Oslo, N-0316 Oslo, Norway*
(Dated: November 12, 2018)

Neutron-rich isotopes in the *sdpf* space with $Z \leq 14$ require modifications to derived effective interactions to agree with experimental data away from stability. A quantitative justification is given for these modifications due to the weakly bound nature of model space orbits via a procedure using realistic radial wavefunctions and realistic NN interactions. The long tail of the radial wavefunction for loosely bound single particle orbits causes a reduction in the size of matrix elements involving those orbits, most notably for pairing matrix elements, resulting in a more condensed level spacing in shell model calculations. Example calculations are shown for ^{36}Si and ^{38}Si.

I. INTRODUCTION

New facilities for rare isotope beams will push the experimental capabilities of nuclear physics with radioactive beams to more unstable, shorter-lived nuclei. Properties of these nuclei exhibiting different behavior than stable nuclei, like the evolution of shell structure, are of significant interest for the next decades of research. A new theoretical technique and its behavior for stable and exotic nuclei has been studied to examine the importance of refining theoretical approaches for the production of model space interactions for unstable nuclei.

Much research has been done using renormalization methods to convert a realistic interaction fit to nucleon-nucleon (NN) scattering data into an interaction in the nuclear medium. The goal is to renormalize the interaction to valence orbits outside of a stable, semi-magic or doubly magic nucleus treated as a vacuum in further calculations. A typical example would use ^{16}O as the core and renormalize the NN interaction into the *sd* model space. For such an application, the harmonic oscillator basis of the form $\Psi_{nlm_l}(\vec{r}) = R_{nl}^{HO}(\mathrm{r}) \, Y_{lm_l}(\theta,\phi)$ is generally used. Additionally, all the valence orbits are bound in the harmonic oscillator basis. For more exotic closed-subshell nuclei, loosely bound orbits often play a role. The harmonic oscillator basis is less applicable further from stability. Loosely bound orbits particularly deviate from the oscillator basis, as they exhibit a "long-tail" behavior with a larger spread in the radial wavefunctions. However, few calculations have been done with a realistic radial basis for unstable nuclei with renormalized NN interactions.

Experimental interest in neutron-rich silicon isotopes and the failure of some shell model Hamiltonians to reproduce data in the region have led to modifications in the SDPF-NR interaction [1], which had been the standard for shell model calculations in the *sdpf* model space. The new SDPF-U interaction has different neutron-neutron pairing matrix elements for $Z \geq 15$ and $Z \leq 14$ to account for the behavior of *pf* neutron orbits relative to the number of valence protons. The $Z \leq 14$ version of the interaction treats neutron-rich unstable nuclei that exhibit different shell behavior than the less exotic nuclei in the $Z \geq 15$ nuclei. The interest in silicon isotopes and the nature of the SDPF-U interaction make ^{34}Si a suitable choice for the renormalization procedure with a realistic basis. A similar effect occurs for the neutron-rich carbon isotopes around the $N = 14$ closed subshell, requiring a 25% reduction in the neutron-neutron two-body matrix elements from the effective interactions derived for the oxygen isotopes [2].

II. RENORMALIZATION PROCEDURE

We begin with the realistic charge-dependent NN interaction N^{3}LO derived at fourth order of chiral perturbation theory with a 500 MeV cutoff and fit to experimental NN scattering data [3]. The N^{3}LO interaction is renormalized using a similarity transformation in momentum space with a sharp cutoff of $\Lambda = 2.2$ fm^{-1} to obtain the relevant low momentum interaction [4]. We will refer to this technique as a v_{lowk} renormalization. Skyrme Hartree-Fock calculations are performed with the Skxtb interaction [5] for a chosen closed sub-shell target nucleus to determine the binding energy, single particle radial wavefunctions, and single particle energy spectra for neutrons and protons of the target nucleus. The low momentum interaction is then renormalized into a model space of interest using Rayleigh-Schrödinger perturbation theory [6] to second order including excitations up to $6\hbar\omega$, summing over folded diagrams to infinite order. We will compare three options for the renormalization to produce an effective interaction: harmonic oscillator single particle energies and wavefunctions (HO), Skyrme Hartree-Fock single particle energies and wavefunctions (SHF), and Skyrme Hartree-Fock single particle energies and harmonic oscillator single particle wavefunctions

TABLE I: Single-particle energies for ^{34}Si and ^{40}Ca using the Skxtb interaction. Values in bold are in the model space.

nl_j	^{34}Si proton	^{34}Si neutron	^{40}Ca proton	^{40}Ca neutron
$0s_{1/2}$	-37.73	-32.79	-30.49	-38.18
$0p_{3/2}$	-27.60	-23.10	-22.14	-29.70
$0p_{1/2}$	-22.39	-21.74	-19.03	-26.67
$0d_{5/2}$	**-17.29**	-13.07	**-12.79**	-20.20
$0d_{3/2}$	**-9.08**	-9.03	**-7.23**	-14.65
$1s_{1/2}$	**-13.49**	-10.04	**-8.31**	-15.75
$0f_{7/2}$	-5.97	**-2.62**	-2.68	**-9.89**
$0f_{5/2}$	3.70	**3.33**	4.81	**-2.43**
$1p_{3/2}$	-1.06	**-0.40**	1.44	**-5.48**
$1p_{1/2}$	1.49	**-0.27**	3.27	**-3.66**
$0g_{9/2}$	6.39	9.22	8.63	1.15
$0g_{7/2}$	18.26	18.23	18.76	10.28

TABLE II: Single-particle energies for ^{34}Si and ^{40}Ca in the harmonic oscillator basis. The energy shift is chosen so that the valence energy is identical in both bases. Values in bold are in the model space.

nl_j	^{34}Si proton	^{34}Si neutron	^{40}Ca proton	^{40}Ca neutron
$0s_{1/2}$	-36.93	-34.59	-32.22	-39.21
$0p_{3/2}$	-25.42	-23.09	-21.20	-28.19
$0p_{1/2}$	-25.42	-23.09	-21.20	-28.19
$0d_{5/2}$	**-13.91**	-11.58	**-10.18**	-17.17
$0d_{3/2}$	**-13.91**	-11.58	**-10.18**	-17.17
$1s_{1/2}$	**-13.91**	-11.58	**-10.18**	-17.17
$0f_{7/2}$	-2.40	**-0.07**	0.84	**-6.15**
$0f_{5/2}$	-2.40	**-0.07**	0.84	**-6.15**
$1p_{3/2}$	-2.40	**-0.07**	0.84	**-6.15**
$1p_{1/2}$	-2.40	**-0.07**	0.84	**-6.15**
$0g_{9/2}$	9.11	11.44	11.86	4.87
$0g_{7/2}$	9.11	11.44	11.86	4.87

(CP).

The CP basis and HO basis give identical results to first order in perturbation theory since they use identical wavefunctions. The energies, which are different in the two procedures, come into higher order diagrams via energy denominators, as discussed in [6]. Therefore, the last option is a core-polarization basis (CP basis) since the core-polarization diagrams are affected to leading order even though the result at first order is unchanged.

Skyrme Hartree-Fock radial wavefunctions, once solved, are implemented in the renormalization by using an expansion in terms of the harmonic oscillator basis via:

$$\psi_{nlj}^{SHF}(\vec{r}) = \sum_n a_n R_{nl}^{HO}(r)[Y_l(\theta,\phi) \otimes \chi_s]_j, \qquad (1)$$

where a_n^2 gives the percentage of a specific harmonic oscillator wavefunction component in the Skyrme Hartree-Fock wavefunction. The Skyrme Hartree-Fock wavefunctions and single particle energies can only be determined for bound states. For unbound orbits, the harmonic oscillator basis remains in use, but the Gram-Schmidt process is used to ensure orthonormality of the single particle wavefunctions. The effective interaction, consisting of the derived two-body matrix elements and the Skyrme Hartree-Fock single particle energies, can then be used in a shell model program directly.

III. APPLICATION TO SDPF MODEL SPACE

Neutron-rich silicon isotopes present an interesting application of the procedure outlined in the last section. A deeper understanding of the need for multiple interactions in the $sdpf$ model space, as seen by the form of SDPF-U, can be gained by performing the renormalization for the same model space in multiple ways. The model space chosen is the sd proton orbits and pf neutron orbits. The renormalization procedure is done using all three options for two different target nuclei, producing a total of six interactions. The two target nuclei chosen are the stable ^{40}Ca doubly magic nucleus, and the neutron-rich ^{34}Si semi-magic nucleus. Single particle energies of the SHF basis, using the Skxtb interaction, are presented in Table I for both target nuclei. For an SHF state that is unbound, the radial wavefunction is approximated by a state bound by 200 keV that is obtained by multiplying the SHF central potential by a factor larger than unity. The energy of the unbound state is estimated by taking the expectation value of this bound state wavefunction in the original SHF potential.

In the SHF basis, the calculation of single particle energies shows that the proton orbits are shifted down in energy for ^{34}Si relative to ^{40}Ca, while the neutron orbits are shifted up. For the valence neutrons, this shift results in a switch from four orbits for ^{40}Ca bound by 5.4 Mev on average to four orbits for ^{34}Si centered at 0.0 MeV. This change, specifically the loosely bound energies of the $p_{3/2}$ and $p_{1/2}$, has a significant effect on the wavefunctions, which will be discussed in more detail later. For comparison, the single particle energies used in the HO basis are given in Table II. The Blomqvist-Molinari formula [7] $\hbar\omega = (45A^{-1/3} - 25A^{-2/3})$ MeV gives 11.508 MeV for $A = 34$ and 11.021 MeV for $A = 40$. The absolute value of the harmonic oscillator basis is irrelevant, as only energy differences come into the diagrams in Rayleigh-Schrödinger perturbation theory. For a better comparison to the SHF basis, the absolute value is chosen separately for protons and neutrons such that $\sum_1^{n_{val}} (2J+1)\epsilon_\alpha$ is identical in the HO and SHF bases, where n_{val}, the number of valence orbits, is three for protons
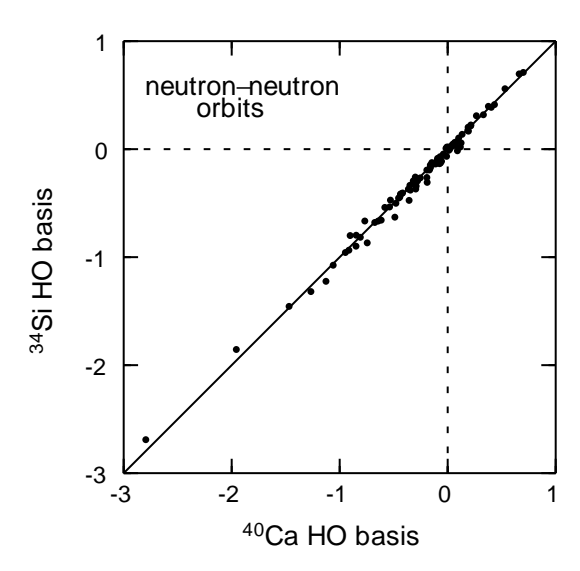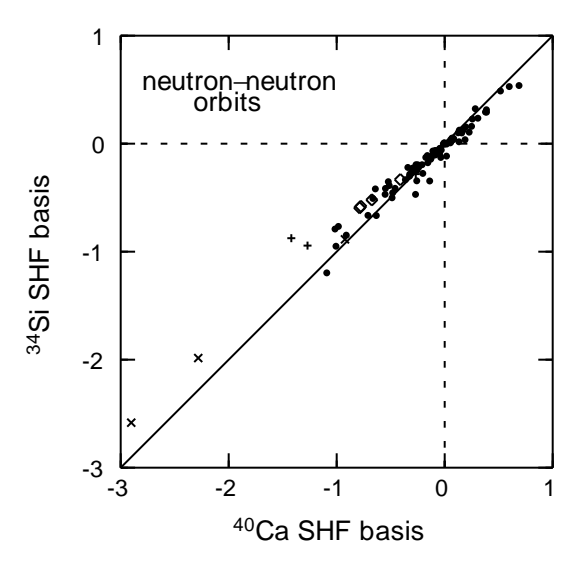
FIG. 1: Comparison of pf neutron-neutron matrix elements (in MeV) for the renormalization procedure in the HO basis for the two target nuclei. The solid line $y = x$ denotes where the matrix elements would be identical.

FIG. 2: Comparison of pf neutron-neutron matrix elements (in MeV) for the renormalization procedure in the SHF basis for the two target nuclei. The solid line $y = x$ denotes where the matrix elements would be identical. Black dots correspond to matrix elements with $J > 0$, while the $J = 0$ matrix elements are split into three groups: $ff - ff$ (crosses), $ff - pp$ (diamonds), and $pp - pp$ (plus signs).

and four for neutrons and ϵ_α is the energy of the single particle orbit given by the $\alpha = n, l, j$ quantum numbers. In order to avoid divergences from the calculation of energy denominators, all model space orbits are set to the same valence energy such that the starting energy [6] of each diagram is constant.
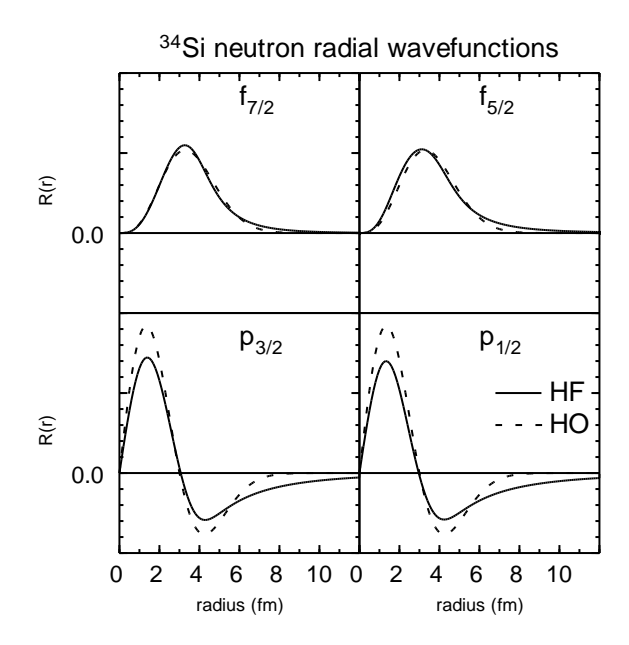

FIG. 3: Comparison of the single particle radial wavefunctions for ^{34}Si in the HO and SHF bases.

Fig. 1 shows a comparison of the pf matrix elements in MeV for both target nuclei with the HO basis used in the renormalization procedure. The values deviate slightly from the line of equality but agree well with each other. Therefore, the choice of target nucleus, whether ^{34}Si or ^{40}Ca, has little effect on the matrix elements in the HO basis. However, when we look at Fig. 2, where the comparison is for both target nuclei in the SHF basis, we see a reduction in the strength of the interaction for ^{34}Si. This reduction with ^{34}Si as the target nucleus is due to the weakly bound nature of the pf neutron orbits.

In the SHF basis, the $f_{7/2}$ orbit is bound by 2.6 MeV, and its radial wavefunction agrees well with the harmonic oscillator wavefunction as seen in Fig. 3. The Skyrme wavefunction is expanded in the harmonic oscillator basis up to $n = n_{max}$ and the a_n coefficients are renormalized to ensure that $\sum\limits_{n=0}^{n_{max}} a_n^2 = 1$. For our renormalization procedure, orbits up to $(2n + l) = 9$ are included, which gives $n_{max} = 3$ for the $f_{7/2}$ and $f_{5/2}$ orbits and $n_{max} = 4$ for the $p_{3/2}$ and $p_{1/2}$ orbits. This includes over 99% of the strength for the f orbits, but only 93% and 92% for the $p_{3/2}$ and $p_{1/2}$ orbits respectively. A first order calculation can be done to $n_{max} = 6$ for all orbits, which gives 100%, 98%, and 97% for the f, $p_{3/2}$, and $p_{1/2}$ expansions respectively.

With this procedure, 99% of the $f_{7/2}$ orbit is represented by the R_{03}^{HO} wavefunction. The $p_{3/2}$ and $p_{1/2}$ orbits are only bound by 400 and 269 keV, respectively. The expected harmonic oscillator component R_{11}^{HO} only makes up 80% and 78% of the respective radial wavefunctions. Higher n orbits which extend farther away from the center of the nucleus contribute the remaining

TABLE III: Core polarization and total matrix elements in MeV of the form $\langle aa|V|bb \rangle_{J=0}$ for different renormalization procedures.

a	b		^{34}Si			^{40}Ca		
			HO	CP	SHF	HO	CP	SHF
$f_{7/2}$	$f_{7/2}$	core pol.	-0.449	-0.377	-0.529	-0.637	-0.649	-0.931
		total	-1.855	-1.869	-1.985	-1.957	-1.982	-2.282
$p_{3/2}$	$p_{3/2}$	core pol.	-0.037	0.001	0.010	-0.021	-0.005	-0.015
		total	-1.319	-1.313	-0.944	-1.267	-1.252	-1.270
$p_{3/2}$	$p_{1/2}$	core pol.	0.068	0.082	0.047	-0.038	-0.069	-0.087
		total	-1.456	-1.462	-0.875	-1.469	-1.488	-1.420

strength. The $f_{5/2}$ orbit is unbound by three MeV, but the solution for the Skyrme radial wavefunction is determined by assuming that the orbit is bound by 200 keV. With this method, 97% of the realistic radial wavefunction is given by the R_{03}^{HO} wavefunction. Single particle radial wavefunctions of valence space neutron orbits are shown in Fig. 3 in both the HO and SHF basis. The long tail behavior of the loosely bound p orbits can be seen in the SHF basis, as the wavefunctions have significant strength beyond 8 fm unlike the oscillator wavefunctions.

The $J = 0$ matrix elements in Fig. 2 deviate more from the line of equality, i.e. the pairing matrix elements are reduced for ^{34}Si when the N^{3}LO interaction is renormalized in the SHF basis. The SDPF-U interaction has different neutron-neutron pairing matrix elements for $Z \geq 15$ and for $Z \leq 14$ to account for 2p-2h excitations of the core correctly, depending on whether ^{34}Si or ^{40}Ca should be considered the core [1]. The SDPF-U neutron-neutron pairing matrix elements are reduced by 300 keV for $Z \leq 14$ in order to produce results in better agreement with experimental data. The pairing matrix elements in Fig. 2 are reduced for the ^{34}Si target by 213 keV on average, relative to the case with ^{40}Ca as the target. While the connection here to the Z-dependence in SDPF-U is only suggestive, the change in target mimics the change in core for calculations in the $sdpf$ region, cited by Nowacki and Poves as the cause of their 300 keV reduction [1]. The reduction of 213 keV is due solely to the change in occupation of the $d_{5/2}$ proton orbit, which can affect the single particle energies and radial wavefunctions, as well as the available diagrams in the core polarization. We find that the change in single particle radial wavefunctions plays the most significant role, but are also able to analyze the effect of the core polarization.

Table III isolates a few matrix elements and compares the total matrix elements and the component due to core polarization for both target nuclei in all three bases. The reduction for total matrix elements involving p orbits is dramatic ($\approx 30\%$) and is primarily due to the extension of wavefunction strength to large distances. Kuo et al. [8] noted a reduction of core polarization in the harmonic oscillator basis and used different oscillator parameters to

account for the core nucleons and valence nucleons separately in halo nuclei. While ^{34}Si is not a halo nucleus, the loosely bound p orbits behave in much the same way as the valence nucleons in a halo nucleus. The reduction in core polarization is seen going from the ^{40}Ca target to the ^{34}Si target in any basis in Table III, although the size of the polarization is reduced for nucleons far from the core. As noted in [8], the core interacts less with nucleons far away, so the excitations of the core are reduced. The core polarization for matrix elements solely involving p orbits is under 100 keV. We observe that the core polarization can be reduced significantly without the total matrix element changing in the same proportion. For instance, the $\langle f_{7/2}f_{7/2}|V|f_{7/2}f_{7/2} \rangle$ matrix element is only reduced by 5% from ^{40}Ca to ^{34}Si in the HO basis even though the core polarization is reduced by 30%. In the SHF basis, which takes into account the realistic wavefunction, the total matrix element is reduced by 13% even though the core polarization is reduced by 43%. We would prefer to compare matrix elements involving the $p_{3/2}$ or $p_{1/2}$ orbits, but the core polarization becomes very small for loosely bound orbits, skewing percentage comparisons. Ogawa et al. [9] produce results which seem to be consistent with ours, identifying a 10%-30% reduction in nuclear interaction matrix elements involving loosely bound orbits using a realistic Woods-Saxon basis. However, they were limited to comparisons of ratios of matrix elements and did not include core polarization. We show that core polarization suppression and reduction due to spread of the wavefunctions are both important effects which should be included, but do not tell the entire story. The $f_{7/2}$ wavefunction is very similar in the HO and SHF bases, as seen in Fig. 3, and yet the $\langle f_{7/2}f_{7/2}|V|f_{7/2}f_{7/2} \rangle$ matrix element does not follow the same trend as the core polarization component in Table III. Other diagrams which are included at second order are relevant, and the full treatment of the renormalization in a realistic basis, as developed here, is necessary for accurate results. Our improvements enable us to perform calculations for neutron-rich silicon isotopes directly.

IV. CALCULATIONS FOR ^{36}SI AND ^{38}SI

The effect of the different interactions on nuclear structure calculations has been studied as neutrons are added to ^{34}Si. In order to obtain a consistent starting point, the proton-proton and proton-neutron matrix elements of SDPF-U have been used, with proton single particle energies (SPEs) chosen to reproduce those obtained by SDPF-U. Because SDPF-U does not reproduce the binding energy of ^{35}Si, the SDPF-U neutron SPEs have been increased by 660 keV. The six interactions use neutron SPEs that reproduce the values of this modified SDPF-U interaction.

The only difference in the six interactions used in the calculations are the neutron-neutron matrix elements. Calculations have been done in the model space discussed
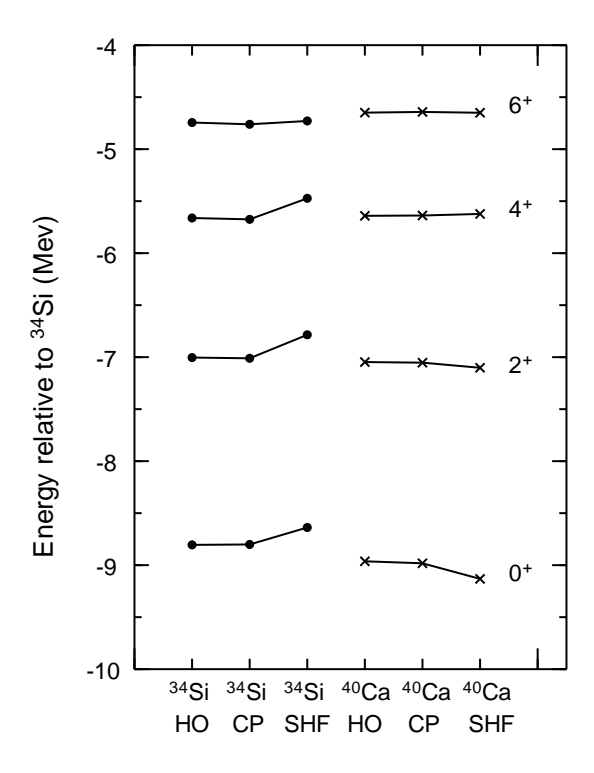
FIG. 4: Calculations for the lowest energy states for $J = 0, 2, 4, 6$ in ^{36}Si relative to ^{34}Si from the renormalization procedure for ^{34}Si and ^{40}Ca, in the HO, CP, and SHF bases for both target nuclei. Crosses are used for calculations with ^{40}Ca as the target nucleus.

FIG. 5: Calculations for the lowest energy states for $J = 0, 2, 4, 6$ in ^{36}Si relative to ^{34}Si using neutron-neutron matrix elements from SDPF-U and the renormalization procedure for both ^{34}Si and ^{40}Ca as target nuclei, using the SHF and HO bases. Experimental data is shown for comparison, with a new mass from [11]. Crosses are used for calculations with ^{40}Ca as the target nucleus.

in the last section with the shell model code NuShellx [10]. Fig. 4 shows the lowest $J = 0, 2, 4, 6$ states in ^{36}Si, relative to ^{34}Si. The HO basis and the CP basis for the same target nucleus deviate by no more than 20 keV. However, the SHF basis noticeably shifts the states, with the largest effect being 170 keV more binding in the ground state with ^{40}Ca as the target nucleus. The binding energy of ^{36}Si changes by nearly 500 keV depending on which renormalization procedure is used. Furthermore, the level schemes for ^{36}Si are more spread out for the crosses where ^{40}Ca is chosen as the target nucleus.

Fig. 5 shows the same states in ^{36}Si relative to ^{34}Si, but now the comparison includes the SDPF-U calculations and experimental data. The CP basis results are not included since they are so similar to the HO basis calculations. We see that the level scheme for ^{36}Si is more spread out for the $Z \geq 15$ SDPF-U calculation than for the $Z \leq 14$ calculation, in agreement with our results discussed above. Our calculations for each method are in reasonable agreement with the comparable SDPF-U calculation, except for the 0^+ state which differs by over 300 keV in both instances. The experimental binding energy relative to ^{34}Si is taken from a new mass measurement of ^{36}Si which is 140 keV higher in energy than previously measured [11]. The excitation energies of the $Z \leq 14$ SDPF-U calculation are comparable to experi-
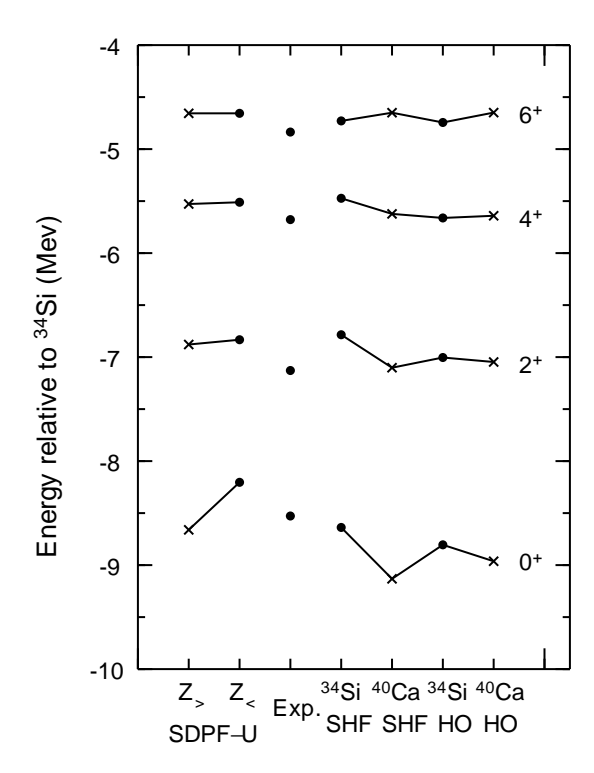
ment, as expected from an interaction fit specifically to neutron-rich silicon isotopes. While no interaction reproduces the experimental data very well, general trends can be seen. The calculations with ^{40}Ca as the target nucleus depicted by crosses result in level schemes that are too spread out in comparison to the experimental data. The reduction in the strength of the interaction for ^{34}Si using the SHF basis results in a reduction of the energy of the states in ^{36}Si, especially for the ground state (the pairing matrix elements were most reduced). The rms between experiment and theory with ^{34}Si as the target nucleus in the SHF basis is 214 keV for the four states shown. One reason for this deviation is the lack of three body forces in the procedure. The inclusion of the NNN interaction, at least via the effective two-body part, is important for a higher level of accuracy. Additionally, the chosen SPEs may contribute to the deviation, which would be better constrained if all the single particle states in ^{35}Si were known experimentally. For exotic nuclei, the calculated single particle state is often above the neutron separation energy and determination of the experimental single particle states may not be possible with current facilities. Thus it is essential to improve energy density functionals such that they provide reliable single particle energies.
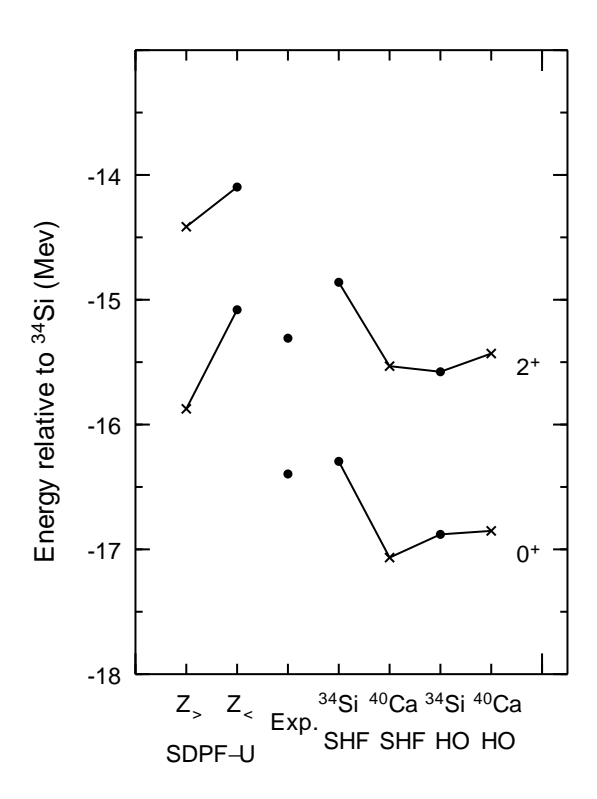
FIG. 6: Calculations for the lowest energy states for $J = 0$ and $J = 2$ in ^{38}Si relative to ^{34}Si using neutron-neutron matrix elements from SDPF-U and the renormalization procedure for both ^{34}Si and ^{40}Ca as target nuclei, using the SHF and HO bases. Crosses are used for calculations with ^{40}Ca as the target nucleus.

The importance of using a realistic basis and an appropriate target nucleus to renormalize an interaction into the nuclear medium for calculations of exotic nuclei is evident from the calculations shown here. Otherwise, the interaction will be too strong and will produce significant overbinding even for the two particle case, an effect

that gets magnified as more particles are added, as seen in Fig. 6 for ^{38}Si. Only the 0^+ and 2^+ states are shown since the 4^+ and 6^+ states are not known experimentally, but the binding energy is only approximately reproduced for the calculations with ^{34}Si in the SHF basis. As noted in the ^{36}Si case, the excitation energy of the 2^+ state is too high in the SHF basis but is reproduced well by the $Z \leq 14$ SDPF-U calculation for ^{38}Si.

V.   SUMMARY AND CONCLUSIONS

The microscopic nucleon-nucleon interaction N^{3}LO was renormalized using v_{lowk} and many-body perturbation theory in order to produce an effective interaction in the nuclear medium that could be used in a shell model code. The renormalization was performed in three different bases: harmonic oscillator, core polarization, and Skyrme Hartree-Fock. The choice of basis can significantly affect the value of matrix elements, as shown in the comparisons of pf neutron-neutron matrix elements for the stable ^{40}Ca and the neutron-rich ^{34}Si nuclei. The difference results from valence orbits being bound by only a few hundred keV, resulting in a long tail in the radial wavefunction relative to the harmonic oscillator wavefunction. The loosely bound orbits cause a reduction in the overall strength of the interaction, an effect that becomes magnified as full scale shell model calculations are performed. Accounting for the properties of the orbits by using a realistic basis is essential for an accurate description of the nuclear interaction in exotic nuclei as determined by the renormalization of an NN interaction.

[1] F. Nowacki and A. Poves, Phys. Rev. C **79**, 014310 (2009).
[2] M. Stanoiu et al., Phys. Rev. C **78**, 034315 (2008).
[3] D.R. Entem and R. Machleidt, Phys. Rev. C **68**, 041001(R) (2003).
[4] S.K. Bogner, T.T.S. Kuo, and A. Schwenk, Phys. Rept. 386 (2003) 1.
[5] B.A. Brown et al., Phys. Rev. C **74** 061303(R) (2006).
[6] M. Hjorth-Jensen, T.T.S. Kuo, and E. Osnes, Phys.

Rept. 261 (1995) 125-270.
[7] J. Blomqvist and A. Molinari, Nucl. Phys. A **106**, 545 (1968).
[8] T.T.S. Kuo et al., Phys. Rev. Lett. **78**, 2708 (1997).
[9] K. Ogawa et al., Phys. Lett. B **464**, 157 (1999).
[10] NuShellX@MSU, B.A. Brown and W.D.M. Rae, http://www.nscl.msu.edu/~brown/resources/resources.html
[11] L. Gaudefroy, W. Mittig, et al., private communication.